

Tailoring the Selectivity for Electrocatalytic Oxygen Evolution on Ruthenium Oxides by Zinc Substitution**

V. Petrykin, K. Macounova, O. A. Shlyakhtin, and Petr Krtil*

The topic of electrochemical gas evolution has shown growing significance in recent years mainly in connection with the anticipated photo(electro)chemical solar energy conversion^[1] or with the development of sustainable chemical technologies. In this respect, hydrogen-evolution (HER) and oxygen-evolution reactions (OER) during the water electrolysis or chlorine-evolution reaction (CER) in chlor-alkali industry^[2] represent the most important processes. Nanocrystalline rutile-type oxides such as RuO₂ and IrO₂ are regarded as benchmark materials for these electrolytic reactions.^[3,4]

Even though oxide electrocatalysts have had practical application for a long time because of their high activity and outstanding stability, a fundamental understanding of their operation, which may lead to a control of the selectivity of the oxide surface towards different oxidation processes, is still lacking. In fact the issue of the selectivity in anodic gas evolution has not been mastered so far because of the difficulty of addressing the nature of the active reaction sites both experimentally and theoretically. A DFT-based thermodynamic description of oxygen- and chlorine-evolution reactions on the (110) rutile surface was reported recently.^[2,5] The theory relates the electrocatalytic activity of the surface to two types of surface oxygen atoms present under conditions of the electrochemical reaction. The first one forms a bridge between two adjacent Ru atoms along [001] direction, and it is believed to be (electro)catalytically inactive. The second type is involved only in one Ru–O bond. It is denoted as coordination unsaturated (O_{cus}). The *cus* oxygen atoms also follow the stacking of cations along [001] direction with metal–metal distance of approximately 3.1 Å, and they are suggested as the active sites for the formation of the key intermediates in both the OER and CER processes. In the

case of the OER, DFT calculations identify a peroxo group formed by two O_{cus} atoms on neighboring Ru atoms as the surface confined intermediate. At the same time, the theoretical analysis predicts this stable intermediate to be the actual active site in the CER process.^[2] This result implies that processes of oxygen and chlorine evolution are strongly correlated, and the selectivity of the surface results from the competition of both processes for the site on the oxide surface. It also suggests that conventional rutile-type oxide catalysts lose their activity for the OER in the presence of chlorides, as chlorine evolution is favored on most of the oxide surfaces.^[2]

Nevertheless, a theoretical description of the active sites for OER and CER can be used to devise electrocatalysts with increased selectivity towards OER in presence of chlorides by selective suppression of the CER. The selectivity of the oxide electrodes may be controlled by varying the particle size and shape^[6] or by a change of the electronic structure of the electrocatalysts by doping.^[7] Keeping in mind the crystal chemistry of rutile structure type^[8] and the effects of heterovalent doping,^[9] one can use these principles to alter the stacking of cations along [001] direction, which eventually should affect the architecture of anticipated active sites. Such a structural change in the doped RuO₂ materials should result in a suppression of chlorine evolution, provided that DFT-based theoretical model is correct.

Herein, the tailoring the structure of the active site described above is given in the first report of the synthesis of active catalysts in Ru–Zn–O system featuring high selectivity to the OER. The evidence of the intended active-site modification is supported by diffraction and X-ray absorption spectroscopy (XAS) data. The voltammetry results combined with differential electrochemical mass spectroscopy (DEMS) data show significant selectivity of the Ru–Zn–O oxides towards the OER even in chloride-containing systems. Ru_{1–x}Zn_xO₂ ($x = 0.0–0.3$) oxide materials were prepared by a spray freezing–freeze drying method.^[10] According to the powder XRD data (provided in the Supporting Information), single-phase Ru_{1–x}Zn_xO₂ materials are formed in the range of $0 < x \leq 0.2$. The impurities of ZnO were identified for zinc contents higher than $x = 0.3$. With an increase of Zn content in Ru_{1–x}Zn_xO₂, the lattice parameters change from $a = 4.4958(2)$ Å and $c = 3.1058(2)$ Å for $x = 0$ to $a = 4.5075(2)$ Å and $c = 3.1062(1)$ Å for $x = 0.2$ owing to the larger size of Zn²⁺ ion (0.74 Å) relative to Ru⁴⁺ (0.62 Å).^[11]

The typical morphology of the prepared powder is presented in Figure 1 ($x = 0.20$). The concentrations of Zn and Ru determined by EDX correspond to $x = 0.19$, which is close to the expected chemical composition of this material; the electron diffraction pattern contains only reflections from

[*] Dr. V. Petrykin, Dr. K. Macounova, Dr. P. Krtil
J. Heyrovsky Institute of Physical Chemistry
Academy of Sciences of the Czech Republic
Dolejskova 3, Prague 18223 (Czech Republic)
Fax: (+420) 286-582-307
E-mail: petr.krtil@jh-inst.cas.cz

Dr. O. A. Shlyakhtin
Department of Chemistry, Moscow State University
Vorobievsky Gory, Moscow 119991 (Russia)

[**] This work was supported by the Grant Agency of the Academy of Sciences of the Czech Republic under contract No. IAA400400906. V.P. acknowledges the support of the Marie Curie International Incoming Fellowship (IIF No. 220711) of the European Commission. The synchrotron measurement time was provided by National Synchrotron Light Source at Brookhaven National Laboratory Project No. 11734.

Supporting information for this article is available on the WWW under <http://dx.doi.org/10.1002/anie.200907128>.

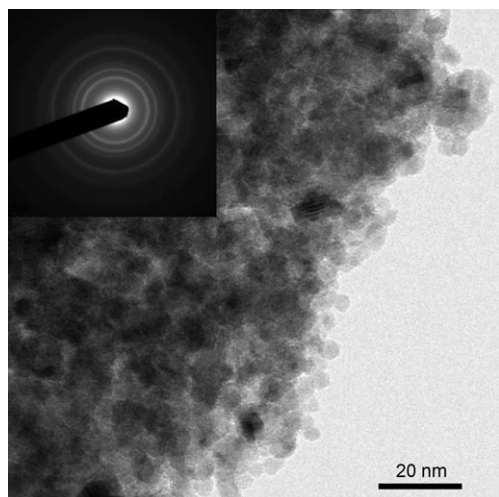


Figure 1. Powder morphology of $\text{Ru}_{1-x}\text{Zn}_x\text{O}_2$ ($x=0.20$) material prepared by a freeze-drying method. Inset: Selected area electron diffraction corresponding to a single-phase rutile-type material.

a rutile-type lattice. To reveal the local structure in the vicinity of Ru and Zn ions, we collected X-ray absorption spectra at Ru and Zn K edges for the synthesized materials and for ZnO reference. The normalized extended X-ray absorption fine structure (EXAFS) functions are presented in Figure 2 for zinc oxide, RuO_2 , and the $\text{Ru}_{1-x}\text{Zn}_x\text{O}_2$ ($x=0.2$) sample, which possesses the highest selectivity towards electrocatalytic oxygen evolution.

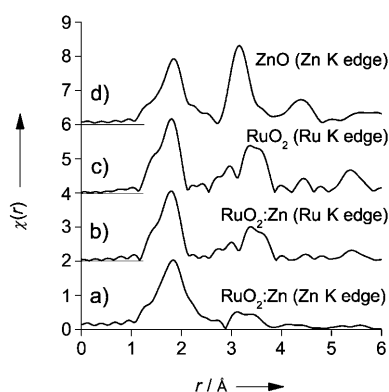


Figure 2. k^2 -normalized EXAFS functions of $\text{Ru}_{0.8}\text{Zn}_{0.2}\text{O}_2$ material at a) Zn K and b) Ru K edges, c) RuO_2 at Ru K edge, and d) ZnO at Zn K edge. For clarity, spectra are offset vertically by two units.

The first peak ($r \approx 1.95 \text{ \AA}$) in all four EXAFS functions corresponds to metal–oxygen coordination in the materials. The second peak at $3.1\text{--}3.2 \text{ \AA}$ is characteristic for the second coordination shell. This shell includes 12 Zn atoms in the close-packed lattice of ZnO or 2 Ru atoms along the [001] direction in the RuO_2 lattice.^[12] Such a difference in coordination numbers accounts for the different peak amplitudes in ZnO and Zn-doped RuO_2 EXAFS functions in Figure 2b–d. The third major peak at around 3.5 \AA in Ru EXAFS spectra of undoped RuO_2 and $\text{RuO}_2\text{:Zn}$ samples corresponds to the next metal–metal coordination shell

including eight Ru(Zn) atoms along the (111) direction of the rutile lattice. Comparison of the data in Figure 2a and Figure 2d rules out the presence of ZnO in the $\text{Ru}_{1-x}\text{Zn}_x\text{O}_2$ ($x=0.2$) material. The significant decrease in the magnitude of the peak at 3.5 \AA in Zn EXAFS spectrum (Figure 2a) relative to that in the Ru EXAFS spectra (Figure 2b,c) indicates a significant deviation from the ideal rutile structure around Zn atoms, similar to that observed for Zn-doped TiO_2 .^[9] Such possible re-arrangement of the crystal structure also manifests itself by splitting of the peak at 3.5 \AA in the Ru EXAFS spectrum. The distortion of the rutile lattice in the vicinity of Zn ions can be linked to oxygen substoichiometry compensating for the different oxidation states of Zn (+2) and Ru (+4). Thus, doping of Zn into RuO_2 lattice breaks the perfect sequence of Ru atoms along the [001] direction and results in the re-arrangement of the neighboring metal atoms in the [111] direction and possibly creates more oxygen vacancies on the surface near Zn ions.

The synthesized powders were deposited onto Ti mesh by sedimentation to fabricate electrodes for the characterization of electrocatalytic properties by voltammetry and differential electrochemical mass spectroscopy (DEMS). It was found that all Zn-doped RuO_2 materials were active catalysts for oxygen and chlorine evolution. The overall electrocatalytic activity of the Ru–Zn–O materials in the chloride containing acid media ($0.1 \text{ M HClO}_4/0.15 \text{ M NaCl}$) was compared with that of nanocrystalline RuO_2 (Figure 3). The data shown in Figure 3 combine the measured current density in the electrochemical cell with its components corresponding to OER and CER contributions calculated from the ratio of DEMS signals of the evolved oxygen ($m/z \text{ 32}$) and chlorine ($m/z \text{ 70}$).^[6] These data clearly reflect the change of the rutile-

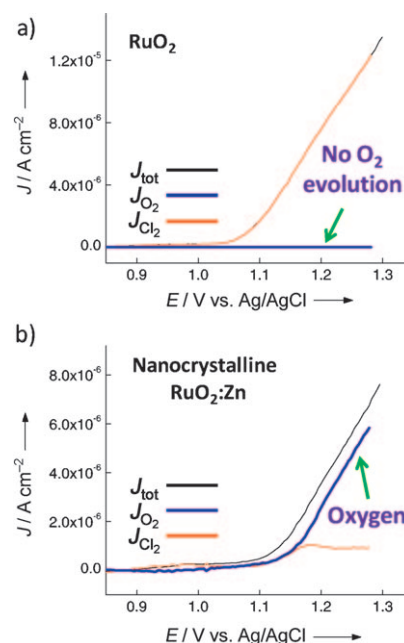


Figure 3. Measured current density (black) and its components corresponding to chlorine (red) and oxygen (blue) evolution during anodic polarization of a) RuO_2 and b) $\text{Ru}_{0.8}\text{Zn}_{0.2}\text{O}_2$ electrodes in $0.1 \text{ M HClO}_4/0.15 \text{ M NaCl}$ solution.

type oxide selectivity from the chlorine evolution (RuO_2) towards oxygen evolution (Ru-Zn-O).

The presence of Zn ions in the rutile lattice most likely prevents the formation of peroxo bridges between the two O_{cus} sites that represent the rate-limiting intermediates for both electrocatalytic processes. In this way, the re-arrangements in the rutile lattice affect the chlorine-evolution process. The oxygen evolution is enhanced, namely, at positive potentials. This behavior suggests an alternative Mars-van Krevelen-like reaction mechanism to take place at more positive potentials,^[13] which seems to be independent of the cations stacking. The fact that the onset of electrocatalytic current on $\text{Ru}_{1-x}\text{Zn}_x\text{O}_2$ is located at more positive potentials (with respect to RuO_2) supports this explanation.

The observed selectivity behavior of the prepared catalysts agrees with the predictions of theoretical model suggested by Hansen et al.^[2] The behavior of the material prepared in the Ru-Zn-O system is rather encouraging in development of catalysts for electrolytic seawater splitting. It also shows the viability of the concept of tailored synthesis of catalysts with predefined selectivity.

Experimental Section

For the synthesis of $\text{Ru}_{1-x}\text{Zn}_x\text{O}_2$ ($x = 0.0\text{--}0.3$) oxides, the appropriate amounts of $\text{Zn}(\text{CH}_3\text{COO})_2 \cdot 2\text{H}_2\text{O}$ (ACS grade, Wako) and Ru nitrosyl nitrate (Alfa Aesar, 31.3% Ru) were dissolved in water, and the total volume was adjusted to obtain a 7 mM solution. The solution (100 mL) was sprayed into liquid N_2 to ensure a high cooling rate. The ice was transferred into the sublimator precooled to -30°C . The sublimation of ice was carried out at 4 Pa according to the following regime: -30°C (1 h), -25°C (3 h), -20°C (4 h), -15°C (6 h), and 30°C (5 h). The obtained fine powder was inserted into the box furnace preheated at 400°C and kept at this temperature for 2 h. The prepared materials were characterized by powder X-ray diffraction (XRD) using Bruker D8 Advance powder X-ray diffractometer with Vantec-1 detector and $\text{Cu}_{\text{K}\alpha}$ radiation. The chemical composition was analyzed by a Hitachi S4800 scanning electron microscope equipped with a Nanotracer EDX detector.

Transmission electron microscopy (TEM) studies were performed with a well-aligned JEM-3010 (JEOL) instrument operating at 300 kV. The $\text{Ru}_{1-x}\text{Zn}_x\text{O}_2$ powders were dispersed in ethanol using an ultrasonic bath. A drop of the obtained solution was transferred onto a Cu microgrid coated with holey carbon film and allowed to dry under ambient conditions. The materials structure and chemical composition was confirmed by electron diffraction and EDX analysis.

X-ray absorption spectra (XAS) were collected at the X18B beam line (Si(111) monochromator) of the National Synchrotron Light Source (Brookhaven National Laboratory). The spectra were measured on pellets containing approximately 40 mg of $\text{Ru}_{1-x}\text{Zn}_x\text{O}_2$ in 200 mg of boron nitride (Aldrich, 98%). In transmission mode on Ru K edge (22117 eV) and Zn K edge (9659 eV). The Zn edge XAS spectra of the material with $x = 0.05$ were acquired in fluorescence mode using a 13-channel Ge detector. All data normalization, smoothing, and background subtraction were performed in the IFEFFIT software package.^[14]

The electrocatalytic activity of the prepared materials was tested with respect to parallel oxygen and chlorine evolution by cyclic voltammetry combined with differential electrochemical mass spectroscopy (DEMS). The electrodes for electrochemical experiments

were prepared from synthesized materials by repeated sedimentation of nanocrystalline powders from a water based suspension onto a Ti mesh (open area 20%, Goodfellow). For this purpose, the initial oxide suspensions were prepared in an ultrasonic bath and contained approximately 5 g L^{-1} of ruthenium-based oxides in MilliQ quality deionized water. The deposition proceeded from an actual volume of 5 mL for 60 s. The deposited layer was dried in air at 100°C for 30 min. The number of the deposition cycles was adjusted to obtain a surface coverage of about $1\text{--}2\text{ mg cm}^{-2}$ of active oxides. The deposited layers were later stabilized by annealing the electrodes for 20 min at 400°C in air followed by slow furnace cooling.

Voltammetric experiments were carried out at the scan rate of 5 mVs^{-1} in a home-made Kel-F single compartment cell with Pt auxiliary electrode and Ag/AgCl reference electrode. The applied potential was controlled by PAR 263A potentiostat. The solutions used for electrochemical experiments (0.1M HClO_4 and 150 mM NaCl in 0.1M HClO_4) were saturated by argon prior to the measurements. The DEMS apparatus used to study the selectivity of nanocrystalline RuO_2 -based anodes consisted of Prisma TM QMS200 quadrupole mass spectrometer (Balzers) connected to TSU071E turbomolecular drag pumping station (Balzers). The DEMS setup was calibrated with respect to oxygen evolution in Cl^- -free environment to evaluate proportionality factor between the current/charge recorded in electrochemical experiment and detector current of the mass spectrometer. The separation of the O_2 - and Cl_2 -related current contributions was based on the O_2 calibration and on the additivity of the current contributions.

Received: December 17, 2009

Published online: May 31, 2010

Keywords: chlorine · electrochemistry · oxygen · ruthenium · solid-state structures

- [1] M. W. Kanan, D. G. Nocera, *Science* **2008**, 321, 1072–1075.
- [2] H. A. Hansen, I. C. Man, F. Studt, F. Abild-Pedersen, T. Bligaard, J. Rossmeisl, *Phys. Chem. Chem. Phys.* **2010**, 12, 283–290.
- [3] S. Trasatti, *Electrochim. Acta* **1987**, 32, 369–382.
- [4] S. Trasatti, *Electrochim. Acta* **2000**, 45, 2377–2385.
- [5] J. Rossmeisl, Z. W. Qu, H. Zhu, G. J. Kroes, J. K. Nørskov, *J. Electroanal. Chem.* **2007**, 607, 83–89.
- [6] J. Jirkovsky, H. Hoffmannova, M. Klementova, P. Krtil, *J. Electrochem. Soc.* **2006**, 153, E111–E118.
- [7] K. Macounova, M. Makarova, J. Jirkovsky, J. Franc, P. Krtil, *Electrochim. Acta* **2008**, 53, 6126–6134.
- [8] C. N. R. Rao, J. Gopalakrishnan in *New Directions in Solid State Chemistry*, Cambridge University Press, Cambridge, **1997**.
- [9] T.-J. Chen, P. Shen, *J. Phys. Chem. C* **2009**, 113, 328–332.
- [10] a) “Cryochemical Synthesis of Materials”: O. A. Shlyakhtin, N. N. Oleynikov, Y. Tretyakov in *Chemical Processing of Ceramics*, Marcel Dekker, New York, **2005**, pp. 77–137; b) R. Forgie, G. Bugosh, K. C. Neyerlin, Z. Liu, P. Strasser, *Electrochem. Solid-State Lett.* **2010**, 13, B36–B39.
- [11] R. D. Shannon, *Acta Crystallogr. Sect. A* **1976**, 32, 751–767.
- [12] V. Briois, S. H. Pulcinelli, C. V. Santilli, *J. Mater. Sci. Lett.* **2001**, 20, 555–557.
- [13] a) M. Wohlfahrt-Mehrens, J. Heitbaum, *J. Electroanal. Chem.* **1987**, 237, 251; b) K. Macounova, M. Makarova, P. Krtil, *Electrochem. Commun.* **2009**, 11, 1865–1868.
- [14] M. Neville, *J. Synchrotron Radiat.* **2001**, 8, 322–324.